Growth and electronic structure of ultrathin epitaxial Pd(111) films on Fe(110) and Co(0001) substrates

D. A. Wesner,* W. Weber, D. Hartmann, and G. Güntherodt
2. Physikalisches Institut, Rheinisch-Westfälische Technische Hochschule Aachen, Templergraben 55, W-5100 Aachen, Federal Republic of Germany

U. A. Effner
Institut für Experimentalphysik, AGR 4 Oberflächenphysik, Ruhr-Universität Bochum, Universitätsstrasse 150, W-4630 Bochum, Federal Republic of Germany
(Received 27 October 1992)

Epitaxial Pd(111) layers on Fe(110) and Co(0001) thick-film substrates atop W(110) are studied using low-energy electron diffraction (LEED), Auger electron spectroscopy, and angle-resolved photoemission with He I, Ne I, and synchrotron-radiation photon sources. Clear LEED patterns obtained for Pd coverages between 0 and 10 atomic layers (AL's) indicate commensurate Pd(111) overlayer structures in both systems. Satellite reflexes for films in the monolayer coverage range indicate long-range coincidences of 10 Pd atoms on 11 substrate atoms along specific directions. Auger peak intensities of overlayer and substrate as a function of film thickness show straight-line segments separated by breaks at the completion of full atomic layers, suggesting layer-by-layer growth up to a Pd coverage of at least 2 AL and no interdiffusion with the substrates. Interface states are identified for monolayer coverages in both systems by observing a saturation of their intensity as a function of film thickness near 1 AL and a vanishing dispersion with the electronic wave-vector component perpendicular to the surface ($k_\perp$). In contrast to bulklike features at higher Pd coverage, the interface states are insensitive to the incident-light polarization (s or p), possibly because of the almost incommensurate structure of the Pd overlayer. The total Pd-induced 4d bandwidth of the monolayer seen in photoemission spectra taken at photon energies near 60–90 eV is approximately 3.5 eV and exhibits noble-metal character, i.e., little intensity near the Fermi level E_F. Monolayer spectral features in both systems show considerable (≥ 1 eV) dispersion with the electronic-wave-vector component parallel to the surface, $k_\parallel$, indicating interactions within the overlayer. All Pd-induced features have mainly overlayer character, i.e., all exhibit a Pd-like photon-energy dependence in the region of the Pd 4d Cooper minimum. The transition to a bulklike Pd(111) electronic structure is virtually complete at a Pd coverage of 5 AL, although dispersion with $k_\perp$ starts at 3 AL and a final-state resonance typical of the bulk is even discernible at 1.5 AL. A "second-layer" interface state for Pd coverages between 1.5 and 2.5 AL probably arises through the changed potential caused by the second Pd layer.

I. INTRODUCTION

Many of the magnetic properties of three-dimensional solids change intriguingly upon transforming to two-dimensional structures such as surfaces or ultrathin films. Examples include the following:

(i) strongly enhanced magnetic moments predicted near a ferromagnetic surface;[1]

(ii) a drastically reduced Curie temperature in thin ferromagnetic films, which depends sensitively on film thickness[2] and on the presence of adsorbate layers;[3]

(iii) induced "artificial" ferromagnetic order due to metastabile, strained superstructures in epitaxial thin films of (normally) nonmagnetic metals;[4] and

(iv) changed magnetic anisotropies in multilayer structures consisting of alternating ferromagnetic and nonferromagnetic layers.[5]

This last property, in particular, has helped to spur the recent interest in multilayer systems such as Co/Pd and Co/Pt, which are promising candidates for high-density perpendicular magneto-optic recording media. The perpendicular anisotropy in such systems can be controlled through variation of the Co layer thickness and film orientation,[5] and a large Kerr rotation at short photon wavelengths has been demonstrated.[6] Empirically, a correlation between the magnetic properties and interface roughness has been noted[7] and this, plus the fact that the relevant layer thicknesses in such structures are often only a few atomic layers (AL's), suggests that the electronic structure right at the interface plays an important role.

Despite this, there were until recently relatively few spectroscopic studies addressing the spin-resolved electronic structure of such interfaces, for example, using spin-polarized, angle-resolved photoemission (ARUPS), the most powerful technique for investigating surface electronic structure.[8–11] This prompted us to begin a detailed study of interfaces of nonferromagnetic metals with ferromagnetic substrates from the point of view of their electronic band structure, using both spin-polarized and spin-integrated ARUPS. Our goal was first to characterize the film systems as well as possible, e.g., as to the

growth mode and overlayer structure, before studying their electronic structure as a function of film thickness with photoemission. Here, the topics that arise include the possible existence of interface states at low coverages, the nature of the observed spectral features (i.e., whether they arise mainly from overlayer or from substrate states), the interactions within the overlayer (e.g., development of a dispersion relation parallel to the interface), the possible existence of spin splittings in the overlayer-induced features (indicating magnetic polarization effects), and, finally, the development of bulklike electronic structure with increasing overlayer thickness. For the first study we chose thin films of Pd and Pt on ferromagnetic Fe(110) and Co(0001) substrates. We recently reported spin-polarized ARUPS results for these systems[8,9] in which we find spin splitting of interface states, indicating a magnetic polarization of the first atomic layer in contact with the substrate. The present paper focuses on the more general questions of overlayer electronic structure as revealed by spin-integrated ARUPS measurements using conventional as well as synchrotron-radiation excitation sources. It concentrates on Pd overlayers on Fe(110) and Co(0001) substrates. After a brief description of the experimental apparatus used, we begin with a discussion of the film structure and growth mode as determined using low-energy electron diffraction (LEED) and Auger electron spectroscopy (AES). The results for the electronic structure obtained with ARUPS then follow.

II. EXPERIMENTAL DETAILS

Two different experimental setups for angle-resolved photoemisison were used in the work. Use of the first system was kindly provided to us by Professor H. Neddermeyer of the Ruhr-Universität Bochum. It consists of an ultrahigh-vacuum chamber divided into sample preparation and measurement areas; the sample, mounted on a long-travel manipulator, can be moved between these areas. In the measurement part of the chamber, a 50-mm mean radius hemispherical electron energy analyzer (VSW Ltd., Model HA-50) is installed on a goniometer allowing rotation about two independent axes. The angular acceptance is $\pm 1°$. The photon source is the toroidal-grating monochromator beamline "TGM-3" at the BESSY synchrotron radiation facility in Berlin. It delivers photon energies $h\nu$ in the range 10–200 eV. A combined energy resolution (photon plus electrons) of $\Delta E \sim 250$ meV for $h\nu \sim 14$ eV up to ~ 30 eV, and $\Delta E \sim 500$–700 meV for photon energies above, was achieved in the experiments described here, the lower limit being set by the energy analyzer. The W(110) substrate was mounted such that photons were incident in the plane containing the surface normal and the [0,0,1] crystal direction, and were polarized in this plane. The angle between the surface normal and the incidence direction of the light was set at either 37° (i.e., mainly s polarized) or 65° (mainly p polarized). A LEED optics for sample characterization was also installed in the measurement section of the apparatus. In the preparation section, which can be isolated from the measurement section below by a gate valve, custom-built, water-cooled, electron-bombardment evaporators were installed, which allow the growth of thin metal films by sublimation from high-purity ($>99.9\%$) pellets. After thorough degassing, operation at a pressure of $\sim 4\times 10^{-10}$ mbar, only slightly higher than the chamber base pressure of $\sim 1\times 10^{-10}$ mbar, was possible. The metals were simultaneously sublimated onto the substrate and onto a nearby quartz microbalance, giving a relative film thickness measurement.

The second apparatus for spin-polarized ARUPS has been described elsewhere,[12] so only a few relevant details will be given here. Characterization of the sample with LEED and AES is possible in this system, the latter method employing a cylindrical mirror analyzer and data collection in the analog dN/dE model. Thin films here are also sublimated from high-purity ($>99.9\%$) metal pellets using two commercial electron-beam sources (Leybold ESV-2) having added water-cooled shielding. A pressure during deposition of $\sim 6\times 10^{-10}$ mbar (at a chamber base pressure of 1–2×10^{-10} mbar) was achieved after degassing of the sources. As in the other apparatus, a relative measure of film thickness is acquired by simultaneous deposition onto the substrate and onto a quartz microbalance. A noble-gas resonance lamp is the photon source; for the work described here it was operated unpolarized with either He or Ne gas, giving photon energies of $h\nu = 21.2$ eV (He I) or 16.85 eV (Ne I). Photons are incident at an angle of 30° to the surface normal. The 50-mm mean radius hemispherical analyzer is backed by a 100-kV Mott detector to determine the spin polarization of the emitted photoelectrons by scattering from a thin (1500 Å) Au foil; for the spin-integrated spectra described below the unscattered transmitted beam was used. The analyzer was operated at an energy resolution of 100 meV and at an angular acceptance of $\pm 3°$.

III. RESULTS AND DISCUSSION

A. Film growth, characterization, and thickness calibration: AES and LEED

A prerequisite for the study of the electronic structure of the film systems is an understanding of the growth process. This includes knowledge of the film thickness, of the presence of possible defects such as islands, clustering, or interdiffusion with the substrate, and of the overlayer structure (e.g., whether the overlayer is crystalline or not and whether an epitaxial relationship to the substrate is present).

The "substrates" Fe(110) and Co(0001) used in this work were, in fact, epitaxial films about 15-AL-thick grown on a W(110) substrate. More details of these epitaxial systems can be found in the literature.[13] Distortions of the Fe or Co overlayers on W(110) due to misfit to the substrate occur for the thinnest films. At least for the first few layers, the growth mode is layer by layer. For film thicknesses above 6 AL (for Fe) or 4 AL (for Co) the structural distortions are no longer visible in LEED, and a bulklike structure is assumed. For this work, elevated substrate temperatures during overlayer growth

of 150 °C for Fe and 100 °C for Co yielded films having distinct LEED patterns comparable in intensity and sharpness to those of the substrate. To within experimental accuracy, the LEED patterns of the 15-AL Fe or Co films were characteristic of the primitive (1×1) surface structure expected for bulk samples (see, however, the discussion of Pd/Co below).

Pd deposition onto either Fe or Co substrate films was always at room temperature and at low growth rates of ~0.2 AL/min in order to minimize any possible interdiffusion. The growth mode was studied by measuring the intensities of Auger signals of Pd and substrate as a function of film thickness (as measured with the quartz microbalance), and searching for break points separating straight-line segments. These points indicate the completion of full atomic monolayers, provided, of course, the growth is actually layer by layer.[14] Experimentally, deposition of Pd was periodically interrupted and the sample brought to the Auger analysis position by a rotation. In this way the analysis position was very reproducible, and sufficiently many intensity measurements (ca. 15 per AL) could be made to ensure that the results were statistically significant. An example for Pd growth on Fe is in Fig. 1, showing the intensity of the Fe 47-eV, the Pd 330-eV, and the Fe 703-eV Auger lines as a function of Pd film thickness. The intensity of the Fe 47-eV Auger line has a distinct break point corresponding to completion of the first atomic layer, suggesting layer-by-layer growth for at least the first two atomic layers in this system. Assuming this is the case, the inelastic mean free path (IMFP) of the Fe Auger electrons can be estimated from the observed ratio of the slopes of neighboring straight-line segments using the relation

$$\frac{m_{n+1}}{m_n}=e^{-(d/\lambda\cos\alpha)} .$$

Here, m_n is the slope of the nth straight-line segment of the Fe Auger signal, λ is the IMFP of the Auger electrons, d is the thickness of one atomic layer of Pd, and α is the emission angle of the Auger electrons ($\alpha=42°$ for the experimental geometry used). Using $d=2.25$ Å, the interlayer spacing for bulk Pd(111) lattice planes, yields $\lambda\approx3$ Å, a reasonable value for this kinetic energy, when compared to the data compilation and "universal curve" for the IMFP given by Seah and Dench.[15] In contrast to the intensity of the Fe 47-eV Auger line, that of the Pd 330-eV Auger line has less distinct break points. Although these data points in Fig. 1 are shown with a series of fitted straight-line segments, the intensity can equally well be fitted by an exponential curve of the form

$$I(\text{Pd 330 eV})\propto1-e^{-(d/\lambda\cos\alpha)} ,$$

with $\lambda=6$ Å. Note that this value of λ agrees with the IMFP at this kinetic energy given by Seah and Dench.[15] For a deviation from layer-by-layer growth (e.g., clustering), one expects a value of λ from such a fitting procedure that is significantly larger than the IMFP given by the universal curve. Thus, the Pd 330-eV Auger intensity is also consistent with layer-by-layer growth up to a Pd coverage of 2 AL. Experimentally, of course, break points become harder to discern as the change in slope between neighboring straight-line segments decreases with increasing IMFP. The intensity of the Fe 703-eV Auger line is an extreme example: it has a much gentler dependence on Pd overlayer thickness than that of either of the other two lines, without discernible break points. This is because of the significantly longer IMFP [~11 Å (Ref. 15)] for these higher-energy electrons. Similar results obtained for the growth of Pd on Co also imply layer-by-layer growth for up to two atomic layers in that system.

These AES measurements thus give us, along with an indication of the growth mode, an absolute measure of the Pd film thickness. This allows a calibration of the quartz microbalance results, which can then be used for further thickness measurements. Because of the various uncertainties involved, we estimate an error in such film thickness measurements of at least $\pm15\%$.

Auger measurements were possible in the second apparatus described above, but not in that at the synchrotron radiation source. There we relied on relative thickness measurements from a quartz microbalance. The calibration is in this case by reference to the photoemission results as a function of Pd film thickness d from both apparatus at comparable photon energies. The valence-band photoemission energy distribution curves (EDC's), as we shall see below, depend sensitively on d.

Low-energy electron diffraction results for the two film systems Pd/Fe(110) and Pd/Co(0001) revealed quite different behaviors. The former has been studied extensively in the past.[16] The Pd layers grow in nearly undistorted epitaxial (111) planes on the Fe(110) substrate in the so-called "Kurdjumov-Sachs" arrangement.[17] One can view this as follows. The starting point is a (111) overlayer of Pd having the bulk Pd lattice constants and oriented with its fcc $[0,1,\bar{1},1]$ crystal direction parallel to the bcc [0,0,1] direction of the Fe(110) substrate. This results in an incommensurate layer with relatively large direction-dependent misfits. If the Pd(111) layers are distorted from their bulk lattice constants only slightly (a compression of $\sim1\%$ and a change in the lattice angle of

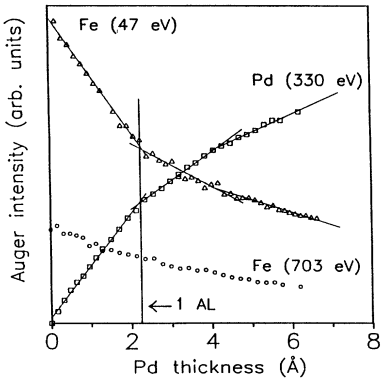

FIG. 1. The intensity of Auger lines (peak-to-peak heights) vs film thickness for Pd growth on Fe(110).

$\sim 1°$), and are rotated azimuthally on the substrate by 5.25°, a commensurate overlayer results. This layer has a 1:1 coincidence along bcc $\langle 1,1,3 \rangle$ directions, and a 10:11 coincidence (i.e., 10 Pd on 11 Fe atoms) along bcc $\langle 1,1,1 \rangle$ directions. The resulting Pd overlayer structure has a large rectangular unit cell containing 10 Pd atoms, so that on average only one Pd atom in 10 is on an Fe(110) lattice point. If one assumes that these Pd atoms are in on-top sites, then the remaining nine atoms are in various (distorted) bridge adsorption sites. Experimentally, the 10:11 coincidence appears in LEED as satellite reflexes along the appropriate reciprocal-lattice directions, beginning at the lowest Pd overlayer thicknesses. These are shown in the photograph of the LEED pattern in Fig. 2(a). Two domains are present, corresponding to rotations of the Pd overlayer by $\pm 5.25°$. The satellite reflexes diminish with increasing Pd overlayer thickness; at 5 AL's they are gone, but two fcc (111) domains remain. Even for this relatively thick Pd overlayer, and for even thicker layers up to ~ 10 AL's the (1×1) LEED reflexes are sharp and distinct.

Palladium overlayers on Co(0001) have a different structure. In this system the symmetry of the overlayer matches that of the substrate, but the bulk lattice constant misfit is relatively large (9.6%). At a coverage of 1 AL, a distinct (1×1) LEED pattern having additional (11×1) superlattice reflexes along the Co $[\bar{1},2,\bar{1},0]$ direction is observed [Fig. 2(b)]. This is consistent with a distorted Pd(111) overlayer. A slight distortion in the Co $[\bar{1},2,\bar{1},0]$ direction yields a 10:11 coincidence corresponding to 10 Pd atoms on 11 Co atoms, while along the Co $[1,0,\bar{1},0]$ direction a relatively large compression (5%) of the bulk Pd(111) lattice constant is required to give a 1:1 coincidence. No superlattice reflexes appear in the other two directions of the Co surface equivalent to $[\bar{1},2,\bar{1},0]$. This is an indication that the Co(0001) substrate is not perfectly hexagonal, but rather retains a slight bcc distortion induced by W(110). The Pd overlayer thus exhibits the "Nishiyama-Wasserman" epitaxial orientation normally observed for fcc (111) overlayer films on bcc (110) substrates.[17] As mentioned above, this slight lattice distortion of Co is not visible in LEED, so that we estimate it is under 1%. For Pd overlayer thicknesses of 2–3 AL's the LEED reflexes become somewhat unsharp and the superlattice reflexes gradually fade. This is probably due to relaxation of the distortion along the Co $[1,0,\bar{1},0]$ direction by incorporation of lattice defects. At higher coverages of up to ~ 10 AL's the superlattice reflexes disappear, and the remaining LEED reflexes become sharper. Analysis of the pattern shows that there is almost no compression in the Co $[1,0,\bar{1},0]$ direction, so that the structure at this stage is nearly the ideal fcc (111) with bulk Pd(111) lattice constants.

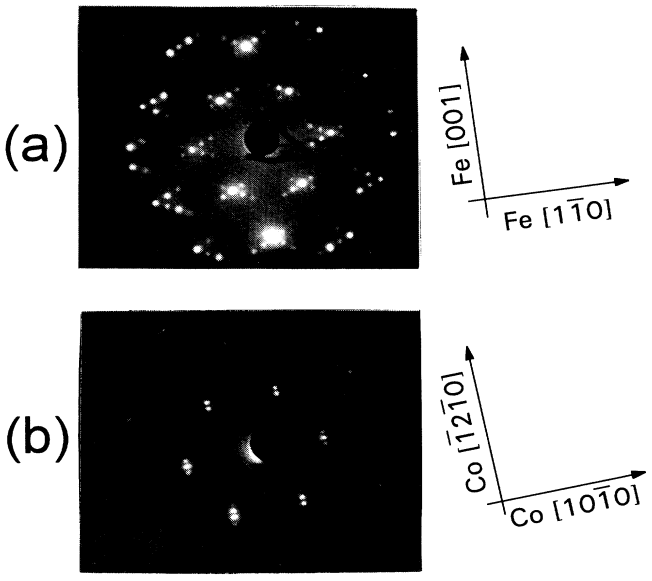

FIG. 2. LEED patterns of (a) 1.5-AL Pd on Fe(110) (electron energy: 170 eV) and (b) 1-AL Pd on Co(0001) (electron energy: 139 eV). Symmetry directions of the substrate are indicated to the right of each pattern.

B. Thickness-dependent electronic structure: interface states

To gain an overview of the electronic structure of the film systems, we first measured photoemission EDC's of the valence band at one photon energy as a function of Pd overlayer thickness. Examples are in Fig. 3(a) for Pd/Fe(110) and in Fig. 3(b) for Pd/Co(0001), both measured with $h\nu = 21.2$ eV. These data are from the second apparatus with the resonance lamp run under identical conditions for each EDC. This allows the comparison of absolute intensities from one EDC to the next. The most obvious result is that even a relatively small amount of Pd, under 1 AL, induces clearly discernible structures in the EDC's. This is understandable, since for this photon energy the atomic photoionization cross section of the Pd $4d$ level is about five times larger than that of the $3d$ level of either Fe or Co.[18] For both systems the EDC's reach an apparent saturation at Pd coverages above ~ 5 AL's, at which point they resemble the spectra of bulk Pd(111) surfaces.[19,20] Before this stage, the EDC's are dominated by a structure at -1.5-eV binding energy [for Pd/Fe(110)] or at -1.3 eV binding energy [for Pd/Co(0001)]. These peaks are clearly separate from those of the substrate and from the Pd(111) bulk structures that appear first at larger Pd coverage. Their intensities increase in the submonolayer coverage region and saturate near 1-AL Pd coverage (the EDC's for 1.5 AL's are plotted with bold lines in Fig. 3). While the intensity at the binding energy of the peak increases with higher Pd coverage in both cases, this is rather due to an increase in the bulklike features than to a continued growth of the peak. This is the behavior expected for an interface state, i.e., a state which exists by virtue of the interface with no clear counterpart in the substrate or overlayer bulk electronic structure. Similar reasoning has been used to identify interface states for Cu/Ru(0001) (Ref. 21) and for Pd/Nb(110).[22]

For both film systems in the Pd coverage range up to ~ 3 AL's there is no strong increase in the photoemission

intensity at the Fermi level E_F as Pd coverage increases. For Co(0001) there is only a small increase, and for Fe(110) there is even a clear decrease. Palladium d bands in the bulk are only partially occupied (effective $4d$ occupation of 9.6), so that in the thin-film systems one might expect an increase in intensity near E_F with Pd coverage, depending, of course, on the nature of the substrate electronic structure near E_F. However, thin films of Pd on metals often exhibit a closed-shell "noble-metal" electronic configuration which can even influence the chemisorption properties of the overlayer, e.g., the H_2 chemisorption properties of a pseudomorphic Pd monolayer on Nb(110).[23] This is especially the case for, e.g., Pd/Al(111),[24] for which one finds for the monolayer only a relatively deep Pd $4d$ level near -4-eV binding energy. This resembles the level observed for Pd dispersed in a Ne matrix,[25] approximating atomic Pd. For Pd adsorbed on transition metals, the levels are apparently more influenced by the hybridization with substrate d levels, so that intensity appears also at lower binding energies. This is the case for both film systems described here. For film thickness around 4 to 5 AL we find a small but distinct Fermi edge in the EDC's, indicating the transition to a bulklike Pd $4d$ occupation.

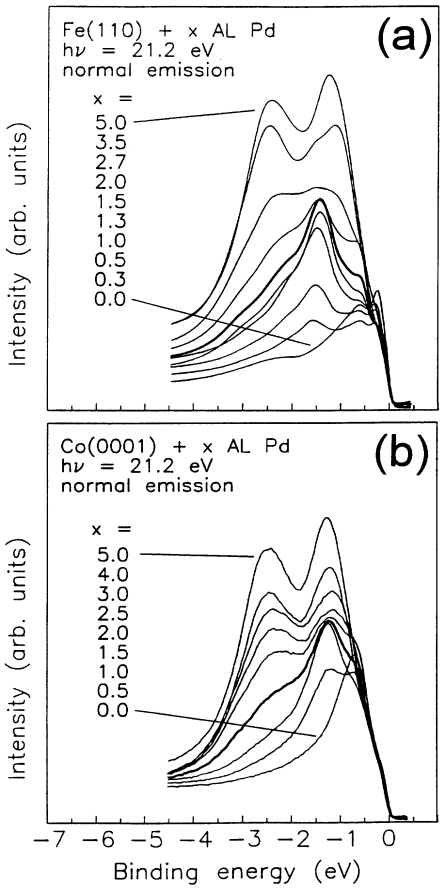

FIG. 3. Valence-band electron energy distribution curves (EDC's) taken at normal emission and $h\nu=21.2$ eV for various Pd overlayer thicknesses (indicated in atomic layers, AL's), plotted on common y axes: (a) Pd/Fe(110), (b) Pd/Co(0001).

C. Monolayer electronic structure: normal emission results with variable $h\nu$

The presence of interface states in these systems raises further questions, especially in relation to our recent spin-resolved photoemission results for these states.[8] We observed that the interface states are spin split, i.e., the interface state peak is seen in both spin-up and spin-down channels, with a peak separation between the channels of about 200 ± 50 meV. The spin splitting in both systems is "inverted", i.e., opposite to the "normal" exchange splitting of the ferromagnetic substrate. Interface states, similarly to surface states, can exhibit differing characteristics. Calculations show, e.g., that the relative contribution of overlayer versus substrate to the state can vary and that the state can be more or less strongly confined to the interface region.[21,22] Such characteristics should influence the magnetic properties of the interface. We set out to address such questions by measuring the electronic states of the monolayer and of thicker films, especially their dispersion relation $E(\mathbf{k})$, where the electronic wave vector $\mathbf{k}$ consists of components parallel and perpendicular to the interface ($k_{\parallel}$ and $k_{\perp}$, respectively).

A further test of the interface-state character of the feature observed to saturate at 1-AL Pd coverage is provided by studies of its despersion with $k_{\perp}$. An interface state should be confined in the direction perpendicular to the substrate, so that no dependence of $k_{\perp}$ is expected. For angle-resolved photoemission at normal emission, $k_{\perp}$ is changed by varying the photon energy. Figure 4 shows EDC's taken with synchrotron radiation in p polarization for the Pd/Fe(110) system. For comparison, Fig. 4(a) shows the uncovered Fe(110) substrate and Fig. 4(b) the results after deposition of 1-AL Pd. Similar spectra for the Pd/Co(0001) system are in Fig. 5, showing clean Co(0001) and its coverage by 1.3-AL Pd. The individual spectra in Figs. 4 and 5 are arbitrarily normalized to all have the same maximum intensity. For clean Fe(110) the results agree with those obtained in similar studies of bulk Fe(110).[26] A peak due to the crossing of two Σ_1 bands appears at $h\nu=16$ eV. One component of this peak disperses by $\sim$300 meV toward E_F as the photon energy increases, while the other component disperses slightly toward higher binding energy and is visible as a shoulder at $h\nu=30$ eV. The range of $k_{\perp}$ represented by the spectra in Fig. 4 is about half the Brillouin zone in the $\overline{\Gamma N}$ direction of Fe. In contrast to this dependence on $k_{\perp}$, the interface state peak in Fig 4(b) shows almost no dispersion (<100 meV), and appears to be nearly unchanged in shape and intensity over most of the photon-energy range. A small dispersion can arise from the error in the setting of the sample angle for normal emission, about $\pm3°$. Similar results obtain for the Pd/Co(0001) system. The substrate EDC's agree with results in the literature,[27] except for the absence of a Co surface state at -0.3-eV binding energy, which, however, is very sensitive to H_2 adsorption. (Hydrogen is the major component of the residual gas in the vacuum system. We, nevertheless, were able to identify the surface state in measurements of Co films made shortly after deposition.) Again, the Pd interface state at -1.3-eV binding energy

is practically unaffected by the change in photon energy. Thus, the interface states exhibit no dispersion with $k_\perp$.

The EDC's for $h\nu=28$ and 30 eV in Fig. 4(b) show, besides the interface state at -1.5-eV binding energy, a second peak at -2.1-eV, which is attributable neither to the substrate nor to a bulklike Pd spectral feature. This peak is visible, if at all, only as a shoulder at the lower photon energies in Fig. 4(b), but at higher photon energies it is comparable in intensity to the -1.5-eV peak. An example is in Fig. 6, which shows normal-emission EDC's for 0.5-AL Pd on Fe(110) at photon energies from 45 to 63 eV taken in p polarization. As in Figs. 4 and 5, the EDC's are normalized to have the same maximum intensity. Both peaks appear in each EDC; no dispersion is evident in either. This second peak also exhibits a saturation in its intensity near Pd coverages of 1 AL, so that it is probably also attributable to the interface. For $h\nu \geq 60$ eV a third peak appears near -4.5-eV; it has no counterpart in the clean Fe(110) EDC, so that we assign it to a Pd-induced state. It is present at the lowest Pd coverages, but overlaps in binding energy a bulklike Pd EDC peak, which appears at higher Pd coverages. All three peaks are also in other EDC's (not shown) at photon energies around 80–90 eV. For these higher energies there is also a very weak structure near -3-eV binding energy. As at all the lower photon energies, no dispersion of any of these peaks with $k_\perp$ is found in these higher photon-energy ranges. One can estimate the total Pd 4d bandwidth for the monolayer by comparing the EDC's of clean substrates with those of monolayer Pd coverages measured over a wide photon energy

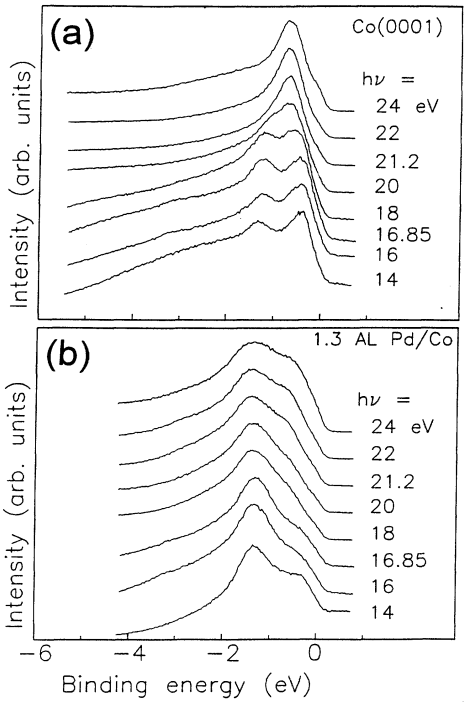

FIG. 5. Similar to Fig. 4, but (a) for clean Co(0001) and (b) after deposition of 1.3-AL Pd.

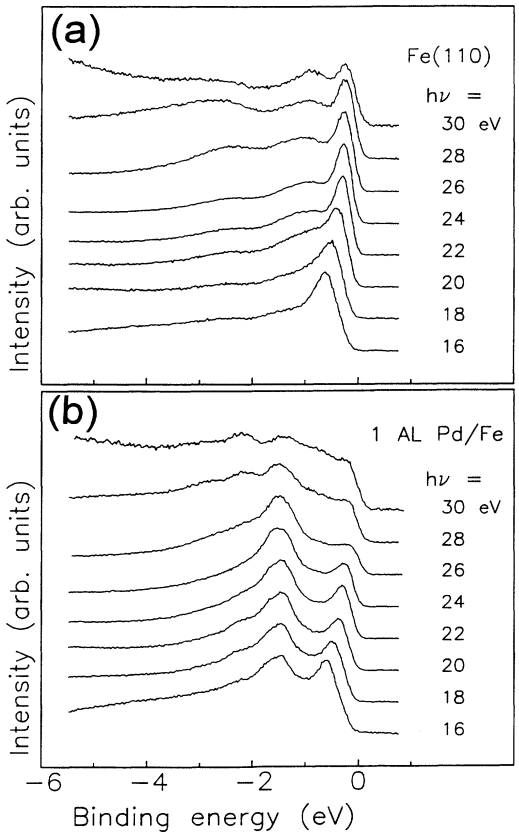

FIG. 4. Valence-band electron energy distribution curves (EDC's), arbitrarily normalized, taken with synchrotron radiation at normal emission and at various $h\nu$ for (a) the clean Fe(110) substrate and (b) after deposition of 1-AL Pd.

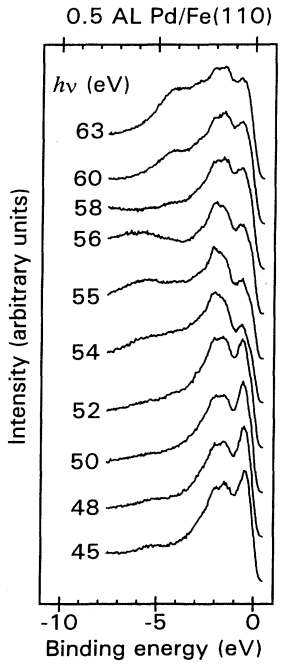

FIG. 6. Similar to Fig. 4, but for the photon energy range from $h\nu=45$ to 63 eV.

range. Such a comparison reveals a total Pd 4*d* bandwidth of about 3.5 eV.

Results surprisingly similar to those for the Pd/Fe(110) system are obtained in normal-emission EDC's for the Pd/Co(0001) system in the photon-energy range from 40 to 80 eV (not shown). In comparison to the Pd/Fe(110) data, only small differences in peak binding energies or in the dependence of peak intensities on photon energy are evident. For example, the second peak appears near a -1.9-eV binding energy and has an appreciable intensity first for photon energies above 40 eV; the third peak is, again, at -4.5 eV, but is visible only for photon energies above 63 eV. The very weak fourth peak is, however, not discernible for Pd/Co(0001). The Pd 4*d* bandwidth is thus also about 3.5 eV for monolayer Pd/Co(0001).

The overall features of the photoemission spectra in Figs. 4–6 are in broad agreement with previous experimental results and calculations for Pd monolayers on transition metals. Angle-resolved photoemission results obtained by El-Batanouny *et al.* showed up to five Pd-induced states in the binding-energy range from -1.5 to -4.1 eV for the commensurate Pd(110) monolayer on Nb(110).[28] In this system the maximum distortion of the nearest-neighbor Pd-Pd distance relative to bulklike Pd(111) planes is about 4%. The highest binding-energy electronic state at -4.1 eV had Σ_1 symmetry, while four states having Σ_1, Σ_3, or Σ_4 symmetry were found at -1.5- to -2.5-eV binding energy. Electronic structure calculations by the same authors agreed well with their observations. Since calculations for a Pd(110) monolayer on Nb(110) did not differ significantly from those of a free-standing bcc (110) Pd monolayer having the appropriate lattice constants, they concluded that the interaction between Pd adatoms and the Nb substrate was relatively weak, probably because the Pd 4*d* states overlap mainly *s*-like Nb bands. Weak coupling to the substrate was thought to be responsible for the relative sharpness of the Pd spectral features. In comparing these results with ours, we find agreement in the total Pd 4*d* bandwidth of approximately 3.5 eV and in the existence and symmetry (see Sec. III D) of the highest binding-energy Pd state. The absence of significant Pd intensity near E_F and the consequent "noble-metal" character of the Pd monolayer is present in both studies. However, in both the Pd/Fe(110) and Pd/Co(0001) systems fewer states are visible in the EDC's, and the lower binding-energy states in the range between -1.3 and -2.1 eV show no clear dependence on light polarization (see Sec. III D). There is also apparently a difference in the photon-energy dependence of the various EDC peaks; all the states of the Pd/Nb(110) system were visible at relatively low photon energies. (El-Batanouny *et al.* used resonance lamp photon energies in their measurements.)

For monolayer Pd(100) on Fe(100), spin-resolved density-of-states calculations by Huang *et al.*[29] show a large degree of 4*d*-3*d* hybridization, which was suspected of causing a distorted spin-resolved electronic structure for the Pd overlayer states in comparison to those of a free-standing Pd(100) monolayer [in contrast to the calculations of Pd on Nb(110) (Ref. 28)]. A total Pd 4*d* bandwidth of about 4 eV and a reduced Pd density of states near E_F are found in this system, in general agreement with our results. However, only layer-resolved densities of states and not *k*-resolved band structures were published, and the Pd overlayer structures in the systems Pd/Fe(100) and Pd/Fe(110) are rather different. [The pseudomorphic Pd(100) monolayer on Fe(100) exhibits a 4.3% lattice expansion relative to bulk Pd(100)]. This makes detailed comparisons with our results difficult. Still, relatively large Pd state densities are predicted near -1- to -2-eV binding energy, approximately where we observe two Pd interface states. The increased hybridization and consequent broadening of spectral features in the EDC's might also be responsible for the inability to observe more Pd-induced states in the Pd/Fe(110) and Pd/Co(0001) systems, relative to Pd on Nb(110).

Experimental results for the Pd(100)/Fe(100) system were also recently reported by Rader *et al.*[11] Spin-resolved normal-emission EDC's of the Pd monolayer taken at $h\nu=21$ eV show Pd-induced intensity from several states in the binding-energy range from -1.5 to -3 eV, which is in rough agreement with the binding energies of the states in this work. (Interface state character, dispersion with $k_\perp$, and $h\nu$ dependence were not reported.) However, the quite different character of the spin-resolved Pd-induced peaks in comparison to our spin-resolved results[8] (especially for the majority-spin channel) raises doubts as to the similarity of the two systems. The amount of Pd character in the Pd-induced structures (see Sec. III E) is also different in the two systems.

D. Light polarization dependence

Most of the measurements in the monolayer Pd coverage range in Figs. 4–6 were repeated for *s*- and *p*-polarized light incidence conditions. Remarkably, the Pd interface state peaks in the binding-energy range from -1.3 to -2.1 eV show no dependence on light polarization in either system (i.e., almost no change in peak binding energy, intensity, or width). Although the experimentally realizable *s* and *p* polarizations are not pure, this cannot explain the behavior, since the substrate states and bulklike Pd(111) states both show clear changes in peak intensities. Moreover, the intensity of the Pd-induced peak near -4.5 eV does depend on light polarization, being enhanced in *p* polarization. According to photoemission dipole selection rules for normal emission,[30] this is consistent with an initial state having Σ_1 [assuming a bcc (110) surface] or Λ_1 [assuming an fcc (111) surface] symmetry.

Density-of-states calculations by Kumar and Bennemann for the Pd/Nb(110) system suggest a possible explanation for the insensitivity of the first and second Pd-induced structures to the incident-light polarization.[31] For Pd coverages above 1 AL on Nb(110) a transition from the pseudomorphic Pd(110) structure to an incommensurate Pd(111) overlayer occurs.[23] These authors used a self-consistent tight-binding scheme to calculate the total and partial Pd 4*d* local density of states (LDOS) for both structures. For the incommensurate structure, of course, the local bonding geometry of Pd and Nb

atoms varies continuously from site to site. For this case, Kumar and Bennemann calculated site-resolved partial LDOS for two representative adsorption geometries: an on-top site and a bridge site. While the total Pd LDOS for both adsorption sites of the incommensurate structure were similar, the partial LDOS [i.e., the LDOS resolved into contributions from the various Pd d orbitals: (xy), $(3z^2-r^2)$, etc.] showed differences. This is reasonable, since the local adsorption site geometry should influence the relative contributions of the directed d orbitals to the bonding. Although neither Pd/Fe(110) nor Pd/Co(0001) are incommensurate, the coincidence lattices have relatively large periodicities; the systems are "almost incommensurate." A large variation in bonding site geometry is present locally, similar to an incommensurate structure. In their band-structure calculations for an isolated Pd(110) monolayer having the appropriate lattice constants for pseudomorphic Pd/Nb(110), El-Batanouny *et al.* found that the low binding-energy Pd states of symmetry Σ_1, Σ_3, and Σ_4 near -1.5- to -2.5-eV binding energy had d orbital characters dominated by (x^2-y^2), (yz), and (xz), respectively.[24] Such directed d orbitals should be influenced by a continuously changing adsorption site geometry, so that in the resultant spectral feature no pure Σ_1 or Σ_3 symmetry, and, consequently, no clear dependence on light polarization remains. This would explain our observations. El-Batanouny *et al.* found that the lowest-lying Pd band near -4.5 eV had Σ_1 symmetry dominated by s character; this band might thus be less influenced by the local adsorption site geometry. In the calculations this state has a nearly parabolic, free-electron-like dispersion relation $E(k_\parallel)$, in comparison to the flatter dispersion relations of the states at lower binding energy, which are probably more localized. In the Pd systems studied here, this deep-lying state is the only Pd monolayer feature for which we find a dependence on light polarization.

E. The electronic character of the overlayer-induced states

Given the presence of interface states in the monolayer electronic structure, we wish to determine to what extent they are associated with substrate or overlayer. The observation of no energy dispersion with $k_\perp$ shows that the interface states are two dimensional, but they could as well be confined to the first few layers of the substrate as to the Pd overlayer. The correlation with Pd coverage could arise through a change in the electronic potential in the substrate induced by the overlayer. In this case, of course, the observation of magnetic polarization of the states would be unsurprising. The photon-energy dependence of the photoionization cross section for the various states involved gives us the possibility to determine their character, i.e., to decide if the states are assignable to Pd or to the substrate, or if they are intrinsically of mixed character.

Calculated atomic photoionization cross sections[18] show that up to $h\nu\sim 40$ eV the cross sections of the Pd $4d$, Fe $3d$, and Co $3d$ atomic states all increase, with the Pd cross section being about 3 to 5 times larger than that of either $3d$ metal. Near $h\nu=40$ eV a decrease in all cross sections sets in, which, however, is much stronger for the Pd state as for Co or Fe. This is due to the presence of a Cooper minimum[32] in the Pd cross section near $h\nu=110$ eV. At the Cooper minimum the $3d$ levels of Fe and Co have a cross section about 20 times that of Pd; the crossover point (corresponding to equal photoionization probability) is near $h\nu=60$ eV. While these are free-atom results, the effect is so large that we expect to find at least the general trend mirrored in solid-state systems. For example, this method was used to determine the relative contributions of individual constituents to the valence-band electronic structure of multicomponent systems such as intermetallic alloys.[33]

Figure 7(a) compares EDC's for 1-AL Pd on Fe(110) measured at $h\nu=60$ eV and $h\nu=110$ eV in p-polarized incident-light geometry, both EDC's having been normalized to have the same maximum intensity. In the EDC for $h\nu=60$ eV the three Pd states are clearly visible at -1.5-, -2.1-, and -4.5-eV binding energies, and the substrate $3d$ peak is present only as a shoulder near -0.5-eV binding energy. At $h\nu=110$ eV there is no sign of the Pd peaks. A comparison to analogous EDC's of the clean Fe(110) substrate [Fig. 7(b)] shows that only Fe-related features are present in Fig. 7(a) at $h\nu=110$ eV. This shows that all three Pd-induced structures do possess Pd $4d$ character. For the pseudomorphic Pd(110) monolayer on Nb(110), such $h\nu$-dependent measurements in a lower photon-energy range (for which the Nb sub-

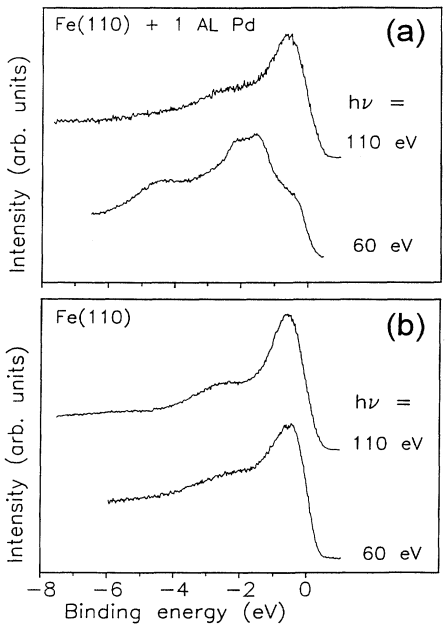

FIG. 7. (a) Valence-band electron energy distribution curves (EDC's) for 1-AL Pd on Fe(110), arbitrarily normalized, taken with synchrotron radiation at normal emission and at $h\nu=60$ and 110 eV. The atomic photoionization cross section ratio $[\sigma(\text{Fe } 3d)/\sigma(\text{Pd } 4d)]$ is ca. 0.8 for $h\nu=60$ eV and ca. 20 for $h\nu=110$ eV. (b) Similar to part (a), but for the clean Fe(110) substrate.

strate exhibits a strongly varying cross section) were also used to determine the character of six structures in the valence-band EDC's.[34] Interestingly, in that system only two of the peaks exhibited pure Pd character, two appeared to be mainly Nb d-like, and two were of mixed character.

For the Pd(100)/Fe(100) system *ab initio* band-structure calculations for the monolayer by Rader *et al.* predict a varying Pd character for the states observed in spin-resolved EDC's at $h\nu=21$ eV.[11] A single minority-spin peak at a calculated binding energy of -1.57 eV is predicted to have 87% Pd character, while in the majority-spin channel several structures are found at calculated binding energies between -2.68 and -0.45 eV, all having reduced Pd characters ranging between 16% and 52%. (These calculated peak binding energies agree well with experimentally observed structures in the EDC's if all calculated binding energies are shifted by 0.5 eV to higher binding energies.) This is interpreted in terms of a spreading of Pd $4d$ majority-spin character among several states because of the increased Pd $4d$-Fe $3d$ hybridization in this channel. Supporting this, majority-spin states with the least calculated Pd content are weak at the photon energy of 21 eV because of the unfavorable photoionization cross section of Fe relative to Pd.[11] The $h\nu$-dependent EDC's reported here for Pd(111) monolayers rule out this explanation in our case. Although we report here only spin-integrated EDC's, such a strong difference in Pd character of the various states (e.g., 16% versus 87%) would be visible even without spin resolution. The EDC's taken in the vicinity of the Cooper minimum (Fig. 7) give no sign of substrate character in the Pd-induced features. This appears to be a genuine difference between the Pd(111)/Fe(110) and Pd(100)/Fe(100) systems. Majority-spin EDC's in the spin-resolved results[8] are also different. Probably the structure of the Pd overlayer plays a more important role than believed in affecting the hybridization between overlayer and substrate.

A further indication of the character of the interface states comes from considering their intensities in the photon-energy range near the photoexcitation threshold of the $3p$ core level of the substrate. The spectra for Pd/Fe(110) in Fig. 6 are in this region; photoexcitation of the Fe $3p$ level to E_F occurs near $h\nu=55$ eV. For several transition metals a resonant satellite structure at $\sim$6-eV binding energy accompanies the $3p$ excitation threshold.[35,36] The satellite structure arises from a multielectron effect in which the photoemission final state has two $3d$ holes bound on the same metal atom site: one $3d$ electron is photoemitted, while the second is promoted to a low-lying excited state. In an atomic picture the two-hole process can be described as[36]

$$3p^6 3d^n 4s + h\nu \rightarrow 3p^6 3d^{n-2} 4snl + e^- ,$$

where nl designates the low-lying excited state. Resonance corresponds to the photon energy being tuned to the $(3p \rightarrow nl)$ excitation, followed by a super Coster-Kronig decay,

$$3p^6 3d^n 4s + h\nu \rightarrow 3p^5 3d^n 4snl \rightarrow 3p^6 3d^{n-2} 4snl + e^- .$$

This leads to the same photoemission final state as the first process. They thus interfere, and both the satellite and the "main line," i.e., the $3d$ states near E_F, exhibit a resonance line shape. The satellite is in most cases enhanced, while the main line shows a dip in intensity or "antiresonance." Such photon-energy dependences were used, e.g., to separate O $2p$ and metal $3d$ contributions to the valence-band spectra of transition-metal oxides.[37] In our case both the clean Fe(110) and Co(0001) surfaces exhibit satellites that resonate near the $3p$ threshold, while the $3d$ peaks near E_F decrease in intensity.

A Pd overlayer reduces the strength of these effects in both systems, but they are still visible in Fig. 6. The satellite appears near resonance in the scans at $h\nu=55$ and 56 eV. In the same region a decrease in the relative intensity of the Fe $3d$ peak near E_F sets in. In contrast, there is no significant change in the intensity of the first Pd interface state at -1.5-eV binding energy upon varying the photon energy through 55 eV. This is consistent with our association of this state with mainly Pd character. The second state at -2.1-eV binding energy is, however, slightly affected. This is seen by comparing the relative peak heights of the first and second peak near resonance: the second peak is enhanced in intensity, reversing the intensity relationship between the two peaks. The same effect is seen for the second Pd peak in the Co system, but there it occurs near the resonance photon energy for Co of $h\nu=60$ eV. This appearance of the effect in the two systems at the resonance photon energy of the substrate suggests a connection with the substrate rather than with something intrinsic to the Pd electronic structure. In part, the relative enhancement of intensity of the peak of Pd/Fe(110) at -2.1 eV is due to the broad background of the satellite peak at higher binding energy. The effect is in any case small in comparison to, e.g., the photon-energy dependence of the satellite intensity from the clean substrate, and the change in relative intensities of the two interface state peaks is much reduced when the Pd coverage is increased from 0.5 to 1 AL. Thus the second Pd-induced peak at monolayer coverage seems also to possess mainly Pd character.

F. Monolayer electronic structure: off-normal results for $E(k_\parallel)$

The dispersion of the monolayer Pd-induced states with $k_\parallel$ was studied in EDC's taken at varying photoelectron emission angles relative to the surface normal along the two symmetry azimuths of the W(110) substrate. Coverages of 1 AL for Pd/Fe(110) and 0.8 AL for Pd/Co(0001) were investigated at photon energies in the range of 18 to 24 eV, for which both the first interface state and the $3d$ states of the substrate are clearly visible. The two-dimensional character of the interface state allows the determination of k for the state by measurement of the photoelectron $k_\parallel$ in the usual manner.[38] The present study shows no evidence for a different $E(k_\parallel)$ dispersion relation for s and p-polarized light incidence. As with the normal-emission results discussed above, Pd-induced features in off-normal EDC's were practically identical for the two light polarizations.

Results for 1-AL Pd on Fe(110) are given in Fig. 8: (a) shows E versus $k_{\parallel}$ for the Pd interface state measured in analyzer scans along the [0,0,1] azimuth, i.e., in the $\overline{\Gamma H}$ direction of the Fe(110) surface Brillouin zone, and (b) shows analogous results for the $[1,\bar{1},0]$ azimuth, i.e., the $\overline{\Gamma N}$ direction. The dispersion of the Fe $3d$ states is confined to the range between E_F and about -1-eV binding energy and does not interfere with the Pd-induced structures. For the $\overline{\Gamma N}$ direction only a slight dispersion of the interface peak, less than about 200 meV, is evident. In the $\overline{\Gamma H}$ direction a total dispersion of about 1.5 eV over the Brillouin zone is evident. The interface state disperses toward higher binding energies, apparently splitting into two branches in the middle of the zone, which merge again near the zone boundary. Near the zone boundary a parabolic dispersion relation symmetric about $k_{\parallel}=1.7$ Å^{-1} holds. This is not far from the value for the Brillouin-zone boundary of bulk Fe(110) in the $\overline{\Gamma H}$ direction, 1.65 Å^{-1}. The difference of 0.05 Å^{-1} may be due to a slight error in the setting of normal emission (less that 2°). In any case, the value for the $\bar{K}$ point of bulk Pd(111), 1.53 Å^{-1}, is evidently inappropriate. [The 5° azimuthal rotation of the Pd(111) plane relative to the substrate in the Kurdjumov-Sachs structure changes the value of $k_{\parallel}$ at the zone boundary by less than 1%]. Thus the overall symmetry of the Pd monolayer on Fe(110), at least that as "seen" by photoemission, is that of a bcc(110) surface.

Figure 9 shows results for 0.8-AL Pd on Co(0001). In this case scanning the analyzer along the [0,0,1] azimuth of W(110) corresponds to the $\overline{\Gamma K}$ direction of the Pd(111) surface Brillouin zone [Fig. 9(a)], while scanning along the $[1,\bar{1},0]$ azimuth of W(110) probes the $\overline{\Gamma M}$ direction of the Pd(111) surface Brillouin zone [Fig. 9(b)]. Unfortunately, experimental constraints prevented the measurement of $E(k_{\parallel})$ out to the zone boundary for the Co(0001) system; the largest value of $k_{\parallel}$ attainable was approximately 1 Å^{-1}. Figure 9 shows results for two photon energies, 18 and 24 eV.

The first observation is that the data points of the interface state (the lowest branch in each azimuth) for the two photon energies fall very nearly on each other. This is an additional test of the nondispersion of the Pd interface state with $k_{\perp}$ and contrasts with the behavior of the Co substrate peaks (the upper branches), whose dispersion with $k_{\parallel}$ is quite dependent on photon energy. The interface state on Co(0001) shows dispersion in both azimuthes of 1 eV or more. In the $\overline{\Gamma K}$ direction the state first disperses upward toward lower binding energy before turning downward at about 0.3 Å^{-1}. In the $\overline{\Gamma M}$ direction the peak disperses continually downward, while a second peak is visible only off normal for $k_{\parallel}>0.2$ Å^{-1}. Off-normal scans for the clean Co substrate show a weak structure somewhat above the region of this second peak, suggesting that it may be due to a state having mixed Pd-Co character. A slight photon-energy dependence

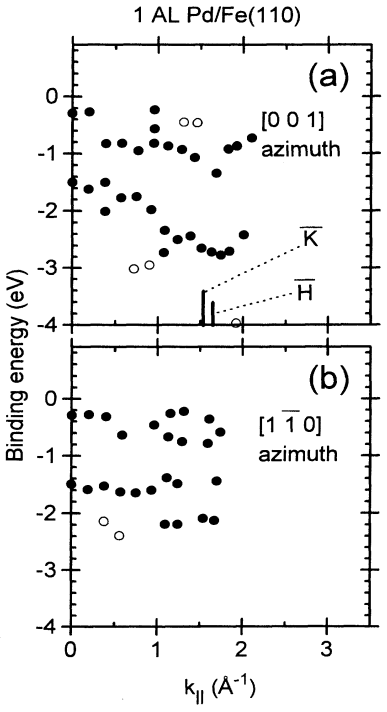

FIG. 8. E vs $k_{\parallel}$ for the Pd interface state of 1-AL Pd on Fe(110): (a) [0,0,1] azimuth [$\overline{\Gamma H}$ of Fe(110) surface Brillouin zone]; (b) $[1,\bar{1},0]$ azimuth ($\overline{\Gamma N}$). All data were taken at $h\nu=18$ eV. Weaker structures are indicated by open symbols.

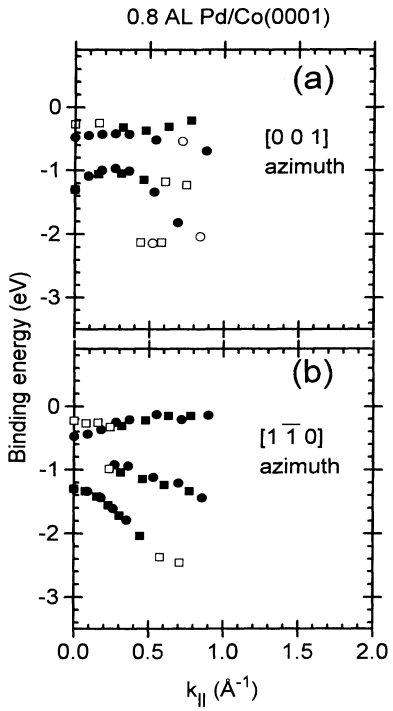

FIG. 9. E vs $k_{\parallel}$ for the Pd interface state of 0.8-AL Pd on Co(0001): (a) [0,0,1] azimuth of W(110) [$\overline{\Gamma K}$ direction of the Pd(111) surface Brillouin zone]; (b) $[1,\bar{1},0]$ azimuth of W(110) [$\overline{\Gamma M}$ direction of the Pd (111) surface Brillouin zone]. Data for both $h\nu=18$ eV (squares) and 24 eV (circles) are combined in the graph, with weaker structures indicated by open symbols.

strengthens this suspicion.

Results for Pd/Co(0001) are qualitatively similar to those for Pd/Fe(110) insofar as both systems exhibit similar maximum dispersions over the surface Brillouin zone of approximately 1 eV. This indicates the development of a two-dimensional $E(k_{\parallel})$ dispersion due to Pd-Pd interactions within the layer. In systems for which little interaction within the adsorbate layer is present, e.g., the random lattice gas previously reported for Pd/Cu(111) at submonolayer Pd coverages,[39] there is almost no dispersion with $k_{\parallel}$. The maximum amount of dispersion we find here agrees well with that observed for Pd/Ag(100) (Ref. 40) or for Pd/Nb(110).[28] In detail, of course, the $k_{\parallel}$ dispersions in the systems Pd/Fe(110) and Pd/Co(0001) discussed here differ both from each other as well as from other Pd overlayer systems previously reported. Probably the structure of the overlayer influences strongly the off-normal dispersion, in spite of the similarities between Pd/Fe(110) and Pd/Co(0001) EDC's at normal emission and higher photon energies that were noted above.

The only extant calculations of $E(k_{\parallel})$ for Pd overlayers reported are for the Pd/Nb(110) system.[28] In addition, Noffke and Fritsche have reported spin-polarized calculations of free-standing Pd(100) layers.[41] Both also agree qualitatively with our results concerning the amount of dispersion, but the band structures differ, of course, in detail. The relatively complex surface structures for the Pd/Fe(110) and Pd/Co(0001) systems present a challenge for electronic structure calculations.

G. Development of bulk electronic structure

To study the transition from the interface-state regime to a bulk Pd(111) electronic structure, we measured normal-emission EDC's in both overlayer systems for $h\nu$ between 16 and 30 eV as the Pd film thickness increased. While similar results hold for both substrates, more Pd thicknesses were measured for the Fe(110) system, so that we show in Figs. 10 and 11 results only for this system. Figure 10 shows spectra for Pd coverages of 1.5 and 2 AL's [parts (a) and (b), respectively], and Fig. 11 shows those for 3 and 5 AL's [parts (a) and (b), respectively]. The photon incidence angle was in all cases 65° to the surface normal, i.e., mainly p-polarized light.

At the lower Pd coverages (Fig. 10) the interface state at -1.5-eV binding energy is still visible, although it is becoming less distinct due to the growth of additional Pd-induced features on either side of it [cf. Fig. 4(b)]. The interface state remains visible even for higher coverages [e.g., it is still discernible as a shoulder in the EDC for 3.5-AL coverage in Fig. 3(a)]. This suggests that it may retain its character as the film thickness increases, instead of rehybridizing with new Pd states. One of the new states seen as the Pd film thickness increases is a broad structure near -2.5-eV binding energy, especially for $h\nu=20$ or 22 eV and for the larger Pd thicknesses. We assign this to a bulklike Pd(111) feature. Measurements on bulk Pd(111) surfaces have revealed a structure at this binding energy in normal-emission EDC's; it is resonantly enhanced at $h\nu=21$ eV.[19,20] The enhancement is believed to be due to a final-state effect: transitions occur from the initial Λ_3 band into a high density-of-states region 18.8 eV above E_F associated with a flat f-like Λ_1 final band.[20] In our data this structure is fully developed for Pd coverages of 3 AL's or more, including its resonant behavior at $h\nu=21$ eV. Remarkably, this resonant character is discernible even at Pd coverages as low as 1.5 AL's [Fig. 10(a)]. Since the final-state band structure of the Fe(110) substrate has no comparable density-of-states feature, this must be due to the development of the bulk Pd band structure perpendicular to the (111) surface, $E(k_{\perp})$. Apparently the final-state electronic band structure high (i.e., ~ 19 eV) above E_F approaches its bulk form even for very thin Pd overlayers.

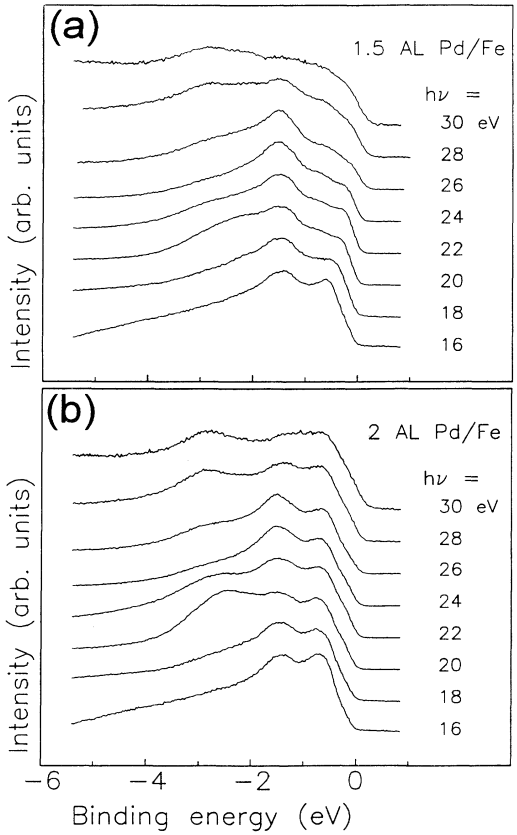

FIG. 10. Valence-band electron energy distribution curves (EDC's), arbitrarily normalized, taken with synchrotron radiation at normal emission and at various $h\nu$ for (a) 1.5-AL Pd on Fe(110) and (b) 2-AL Pd on Fe(110).

A peak is visible near -0.6-eV binding energy for all photon energies at the Pd coverage of 2 AL shown in Fig. 10(b). This structure appears first in the Pd coverage range above 1.5 AL. At a Pd coverage of 1.5 AL [Fig. 10(a)] it is not yet clearly discernible from the Fe $3d$ peak at -0.6 eV. It is seen for coverages up to 2.5 AL; above this coverage range other structures override it. In this regard its behavior as a function of Pd coverage is similar to the saturation of intensity of the interface state at -1.5-eV binding energy with Pd coverage, except that here the peak saturates for a Pd coverage near 2 AL instead of near 1 AL. The spectra in Fig. 10(b) clearly

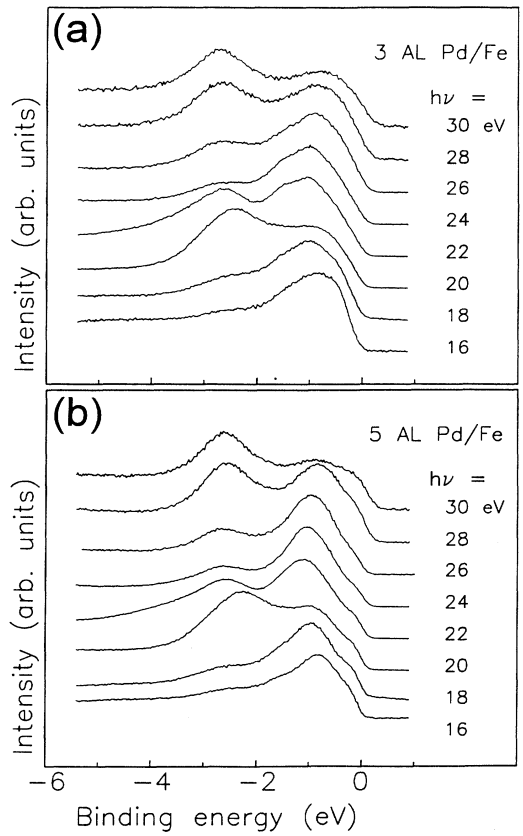

FIG. 11. Similar to Fig. 10, but for (a) 3-AL Pd on Fe(110) and (b) 5-AL Pd on Fe(110).

demonstrate that this peak, like the interface state at −1.5-eV binding energy, shows no significant dispersion with $k_\perp$.

Such a feature was already noted in our previous report of spin-polarized photoemission measurements on the Pd/Fe(110), Pd/Co(0001), and Pt/Co(0001) systems,[8] all three of which exhibit it. In contrast to the spin splitting observed for the interface state of Pd/Fe(110) at −1.5-eV binding energy, one finds for this "second layer" state no shift between the two spin-resolved components of the peak. We believe the most likely explanation of this state is that it is also primarily confined to the interface, consistent with the data in Fig. 10(b), but that the deposition of the second Pd layer leads to a change of the electronic potential, so that the peak appears at a different binding energy. Similar states were seen by Brookes *et al.* in the system Ag/Fe(100), for which interface states were found having discrete binding energies dependent on the number of Ag overlayers.[10] Electronic structure calculations by the same authors support this interpretation, reproducing qualitatively the layer-dependent binding energies for Ag coverages on Fe(100) of 1, 2, and 3 AL. Similar to our data, the interface state for 2 AL appears at lower binding energy relative to that for 1 AL; the 3-AL state is at still lower binding energy. The calculations also show that the 2-AL interface state, while being predominantly centered at the interface, is still slightly less localized than the 1-AL interface state, in that some of its charge density extends into the second Ag layer. If this holds as well for the Pd interface states in our systems, it helps to explain our observation of no splitting for the 2-AL interface state. The magnetic polarization (and, thus, the spin splitting of the photoemission peaks) might be confined to the immediate region of the interface, disappearing for overlayer states that are more delocalized.

The first clear indications of a $k_\perp$-dispersion in the Pd-induced states appear at a Pd coverage of 3 AL [Fig. 11(a)]. At a coverage of 2.5 AL (not shown) the main difference to 2 AL is that the second-layer interface state at −0.6-eV binding energy begins to outweigh that at −1.5-eV; the spectra are still dominated by these two states and by the bulklike resonant peak at −2.5 eV mentioned above. At a coverage of 3 AL the bulk Pd structures begin to dominate the EDC's, although the electronic structure is still not yet that of the bulk Pd(111) surface. At a Pd coverage of 5 AL [Fig. 11(b)] the spectra resemble those of the bulk Pd(111) surface,[19,20] including the $k_\perp$ dispersion of the peak near E_F, although minor changes are present upon further Pd deposition up to thicknesses of 10 AL. The 5-AL Pd coverage is also the first for which the EDC's indicate a Fermi edge, e.g., in the scans for $h\nu = 16$ to 22 eV. This is a photon-energy range for which the substrates [e.g., Fe(110), Fig. 4(a)] show little intensity at E_F. One expects the appearance of a Fermi edge as the Pd overlayer changes from its noble-metal electronic configuration to a more bulklike electronic structure.

The convergence to the bulk electronic structure beginning near an overlayer coverage of 3 AL is in reasonable agreement with theoretical calculations that predict a transition at a coverage of 3–4 AL.[42] The electronic structure for Pd on Fe(110) and Co(0001) appears to converge to the bulk Pd(111) structure more slowly than for Pd on Cu(111). Experiments on the latter system[39] showed the beginning of $k_\perp$ dispersion already at 2.2-AL coverage, at which point a Pd(111) surface resonance also is visible, and the work function of bulk Pd(111) was reached at a coverage of 3 AL. For this system the LEED patterns show pseudomorphic growth up to Pd coverages of 4 AL. Possibly the very different, relatively complex structures observed for Pd overlayers on Fe(110) and Co(0001) affect the transition to a bulklike electronic structure.

IV. SUMMARY

Epitaxial Pd films on Fe(110) and Co(0001) substrates probably grow layer by layer up to film thicknesses of at least 2 AL's. Palladium grows in (111) layers in both systems, but the overlayer structure in both is distorted, with a Kurdjumov-Sachs–type structure holding for Pd/Fe(110) and a Nishiyama-Wasserman structure for Pd/Co(0001). We assume the latter substrate possesses a slight bcc(110) distortion (less than ~1%) induced by the underlying W(110) substrate.

Two interface states in the binding-energy range between −1 and −2 eV and a third structure near −4.5

eV (all measured at normal emission) dominate the electronic structure of the Pd monolayer in both systems. Interface states are identified through the saturation of their intensity near monolayer coverage and through the observation of vanishingly small dispersion with $k_\perp$. These various structures have photon-energy-dependent cross sections, so that not all peaks appear at a given photon energy. The total Pd-induced bandwidth for the monolayer appears to be about 3.5 eV, with little intensity near E_F, as expected for a noble-metal electronic configuration. Only the Pd peak near -4.5-eV binding energy exhibits a dependence on incident light polarization, which may be related to the complex ("almost incommensurate") overlayer structure in both systems. All Pd-induced structures can be shown to have mainly Pd character through the dependence of their intensities on photon energy in the region of the Pd 4*d* Copper minimum. This observation lends support to the interpretation of spin-resolved experiments[8,9] in terms of an induced polarization of the Pd, and not simply the observation of spin-polarized, hybridized electronic states of the ferromagnetic substrates. Palladium overlayers near the monolayer already exhibit a clearly developed dispersion relation with $k_\parallel$, indicating interactions within the film. Such spin-polarized interface states should influence magnetic properties such as the interface magnetic anisotropy.

The transition to a bulklike Pd(111) electronic structure is practically complete for Pd overlayer thicknesses of 5 AL. At this thickness the main EDC peaks resemble those of bulk Pd(111) and a Fermi edge is discernible. However, different features of the electronic structure approach their bulklike state much sooner, e.g., the final-state band structure that causes a resonant structure near $h\nu=21$ eV. Dispersion with $k_\perp$ sets in near a coverage of 3 AL. A second-layer interface state appears at Pd coverages between 1.5 and 2.5 AL, and probably arises from the changed potential in the film upon adding an additional Pd layer.

ACKNOWLEDGMENTS

This work profited from stimulating discussions with P. Baumgart, K.-P. Kämper, and D. Pescia. We are indebted to Professor H. Neddermeyer for the use of his experimental setup at the synchrotron radiation soure BESSY, and to the BESSY staff for their assistance. M. Gruyters, K.-P. Kämper, M. Neuber, and S. Witzel aided us at various stages of the measurements at BESSY. Funding for the work in Aachen came from the Deutsche Forschungsgemeinschaft, Grant GU 193/2-1, and from the Sonderforschungsbereich SFB 341. The Bundesministerium für Forschung und Technologie supported the work at BESSY under Grants No. 05 332 AAI and 05 432 AAB.

*Present address: Lehrstuhl für Lasertechnik, Rheinisch-Westfälische Technische Hochschule Aachen, Steinbachstrasse 15, W-5100 Aachen, Federal Republic of Germany.

[1]A. J. Freeman and C. L. Fu, J. Appl. Phys. **61**, 3356 (1987); C. L. Fu and A. J. Freeman, J. Phys. (Paris) C **8**, 1625 (1988); C. Li, A. J. Freeman, and C. L. Fu, J. Magn. Magn. Mater. **83**, 51 (1990).

[2]U. Gradmann, M. Przybylski, H. J. Elmers, and G. Liu, Appl. Phys. A **49**, 563 (1989).

[3]W. Weber, D. Kerkmann, D. Pescia, D. A. Wesner, and G. Güntherodt, Phys. Rev. Lett. **65**, 2058 (1990).

[4]Z. Celinski, B. Heinrich, J. F. Cochran, W. B. Muir, A. S. Arrott, and J. Kirschner, Phys. Rev. Lett. **65**, 1156 (1990).

[5]C.-J. Lin, G. L. Gorman, C. H. Lee, R. F. C. Farrow, E. E. Marinero, H. V. Do, H. Notarys, and C. J. Chien, J. Magn. Magn. Mater. **93**, 194 (1991).

[6]W. B. Zeper, F. J. A. M. Greidanus, P. F. Carcia, and C. R. Fincher, J. Appl. Phys. **65**, 4971 (1989).

[7]F. J. A. den Broeder, D. Kuiper, A. P. van de Mosselaer, and W. Hoving, Phys. Rev. Lett. **60**, 2769 (1988); P. Krams, B. Hillebrands, G. Güntherodt, K. Spörl, and D. Weller, J. Appl. Phys. **69**, 5307 (1991).

[8]W. Weber, D. A. Wesner, D. Hartmann, and G. Güntherodt, Phys. Rev. B **46**, 6199 (1992).

[9]W. Weber, D. A. Wesner, G. Güntherodt, and U. Linke, Phys. Rev. Lett. **66**, 942 (1991).

[10]N. B. Brookes, Y. Chang, and P. D. Johnson, Phys. Rev. Lett. **67**, 354 (1991).

[11]O. Rader, C. Carbone, W. Clemens, E. Vescovo, S. Blügel, W. Eberhardt, and W. Gudat, Phys. Rev. B **46**, 13 823 (1992).

[12]R. Raue, H. Hopster, and E. Kisker, Rev. Sci. Instrum. **55**, 383 (1984).

[13]For details of Fe(110)/W(110), see U. Gradmann and G. Waller, Surf. Sci. **116**, 539 (1982); H. J. Elmers and U. Gradmann, Appl. Phys. A **51**, 255 (1990). For Co(0001)/W(110), see B. G. Johnson, P. J. Berlowitz, D. W. Goodman, and C. H. Bartholomew, Surf. Sci. **217**, 13 (1989); P. Baumgart, Ph.D. Thesis, Rheinisch-Westfälische Technische Hochschule Aachen, 1989.

[14]C. Argile and G. E. Rhead, Surf. Sci. Rep. **10**, 277 (1989).

[15]M. P. Seah and W. A. Dench, Surf. Interface Anal. **1**, 2 (1979).

[16]P. Baumgart and G. Güntherodt (unpublished).

[17]L. A. Bruce and H. Jaeger, Philos. Mag. A **38**, 223 (1978); E. Bauer, Appl. Surf. Sci. **11/12**, 479 (1982).

[18]J. J. Yeh and I. Lindau, At. Data Nucl. Data Tables **32**, 1 (1985).

[19]F. J. Himpsel and D. E. Eastman, Phys. Rev. B **18**, 5236 (1978).

[20]B. Schmiedeskamp, B. Kessler, N. Müller, G. Schönhense, and U. Heinzmann, Solid State Commun. **65**, 665 (1988).

[21]J. E. Houston, C. H. Peden, P. Feibelman, and D. R. Hamann, Phys. Rev. Lett. **56**, 375 (1986); Surf. Sci. **192**, 457 (1987).

[22]X. Pan, P. D. Johnson, M. Weinert, R. E. Watson, J. W. Davenport, G. W. Fernando, and S. L. Hulbert, Phys. Rev. B **38**, 7850 (1988).

[23]M. A. Pick, J. W. Davenport, M. Strongin, and G. J. Dienes, Phys. Rev. Lett. **43**, 286 (1979); M. Strongin, M. El-Batanouny, and M. Pick, Phys. Rev. B **22**, 3126 (1980); M. Sagurton, M. Strongin, F. Jona, and J. Colbert, *ibid.* **28**, 4075 (1985).

[24]B. Frick and K. Jacobi, Surf. Sci. **178**, 907 (1986).

[25]W. Schrittenlacher, W. Schoeder, H. H. Rotermund, H. Wiggenhauser, R. Grinter, and D. M. Kolb, J. Chem. Phys. **85**, 1348 (1966).
[26]A. M. Turner, A. W. Donoho, and J. W. Erskine, Phys. Rev. B **29**, 2986 (1984).
[27]P. Heimann, E. Marschall, H. Neddermeyer, M. Pessa, and H. F. Roloff, Phys. Rev. B **16**, 2575 (1977); F. J. Himpsel and D. E. Eastman, *ibid.* **21**, 32 007 (1980).
[28]M. El-Batanouny, D. R. Hamann, S. R. Chubb, and J. W. Davenport, Phys. Rev. B **27**, 2575 (1983).
[29]H. Huang, J. Hermanson, J. G. Gay, R. Richter, and J. R. Smith, Surf. Sci. **172**, 363 (1986).
[30]J. Hermanson, Solid State Commun. **22**, 9 (1977).
[31]V. Kumar and K. H. Bennemann, Phys. Rev. B **28**, 3138 (1983).
[32]J. W. Cooper, Phys. Rev. **128**, 681 (1962).
[33]J. F. van Acker, P. W. J. Weijs, J. C. Fuggle, K. Horn, W. Wilke, H. Haak, H. Saalfeld, H. Kuhlenbeck, W. Braun, G. P. Williams, D. Wesner, M. Strongin, S. Krummacher, and K. H. J. Buschow, Phys. Rev. B **38**, 10 463 (1988).
[34]M. El-Batanouny, M. Strongin, and G. P. Williams, Phys. Rev. B **27**, 4580 (1983).
[35]L. C. Davis, J. Appl. Phys. **59**, R25 (1986).
[36]D. Chandesris, J. Lecante, and Y. Pétroff, Phys. Rev. B **27**, 2630 (1983).
[37]R. J. Lad and V. E. Henrich, Phys. Rev. B **38**, 10860 (1988); J. Vac. Sci. Technol. A **7**, 1893 (1989).
[38]E. W. Plummer and W. Eberhardt, Adv. Chem. Phys. **49**, 533 (1982).
[39]M. Pessa and O. Jylhä, Solid State Commun. **46**, 419 (1983).
[40]G. C. Smith, C. Norris, C. Binns, and H. A. Padamore, J. Phys. C **15**, 6481 (1982).
[41]J. Noffke and L. Fritsche, J. Phys. C **14**, 89 (1981).
[42]R. Smith, J. G. Gay, and F. J. Arlinghaus, Phys. Rev. B **21**, 2201 (1980).

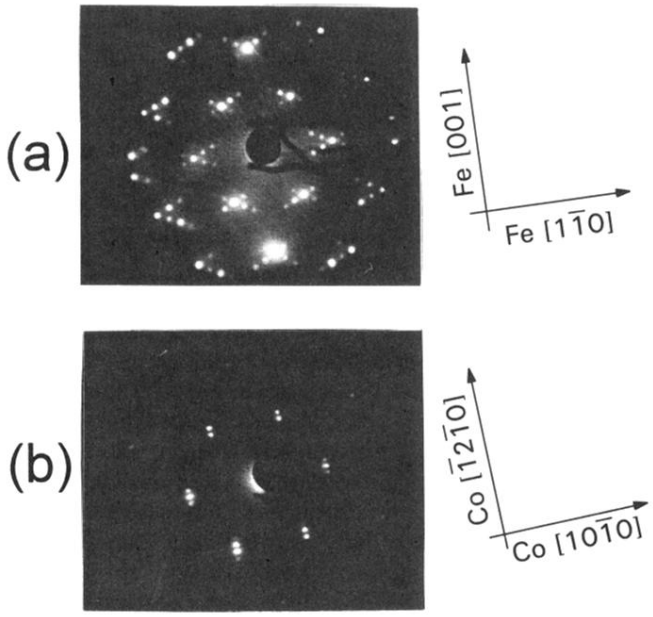

FIG. 2. LEED patterns of (a) 1.5-AL Pd on Fe(110) (electron energy: 170 eV) and (b) 1-AL Pd on Co(0001) (electron energy: 139 eV). Symmetry directions of the substrate are indicated to the right of each pattern.